Mineralogy and Petrology (2006) 86: 63–88
DOI 10.1007/s00710-005-0092-6

Mineralogy and Petrology
Printed in Austria

Gabbroic xenoliths in tuff-breccia pipes from the Hyblean Plateau: insights into the nature and composition of the lower crust underneath South-eastern Sicily, Italy

V. Scribano[1], **G. Sapienza**[2], **R. Braga**[2], and **L. Morten**[2]

[1] Dipartimento di Scienze Geologiche, Università di Catania, Catania, Italy
[2] Dipartimento di Scienze della Terra e Geologico-Ambientali, Università di Bologna, Bologna, Italy

Received December 13, 2004; revised version accepted June 7, 2005
Published online October 12, 2005;
Editorial handling: P. Garofalo

Summary

Crust-derived xenoliths hosted by Miocene basaltic diatremes in the Hyblean Plateau (south-eastern Sicily, Italy) provide new information regarding the nature of a portion of the central Mediterranean lower crust. These xenoliths can be divided into three groups: gabbros (plagioclase + clinopyroxene + Fe–Ti oxides ± apatite ± amphibole ± Fe-rich green spinel), diorites (An-poor plagioclase, clinopyroxene ± Fe–Ti oxides ± orthopyroxene) and mafic granulites (plagioclase + clinopyroxene + green spinel ± orthopyroxene ± Fe–Ti oxides). Gabbros form the main subject of this paper. They represent cumulates whose igneous texture has been locally obliterated by metamorphic recrystallization and shearing. They were permeated by Fe–Ti-rich melts related to tholeiitic-type fractional crystallisation. Incompatible element ratios ($Zr/Nb = 5$–26; $Y/Nb = 1.4$–11) indicate that these cumulate gabbros derived from MORB liquids. Late-stage and hydrothermal fluids caused diverse, sometimes important, metasomatic trasformations. Petrographic and geochemical comparison with gabbroids from well-known geodynamic settings show that the Hyblean lower crustal xenoliths were probably formed in an oceanic or oceanic-continent transition environment.

Introduction

To define the mineralogical and geochemical characteristics and the structure of the lower continental crust, petrologists have studied granulite terrains outcropping on the Earth's surface and lower crustal xenoliths brought to the

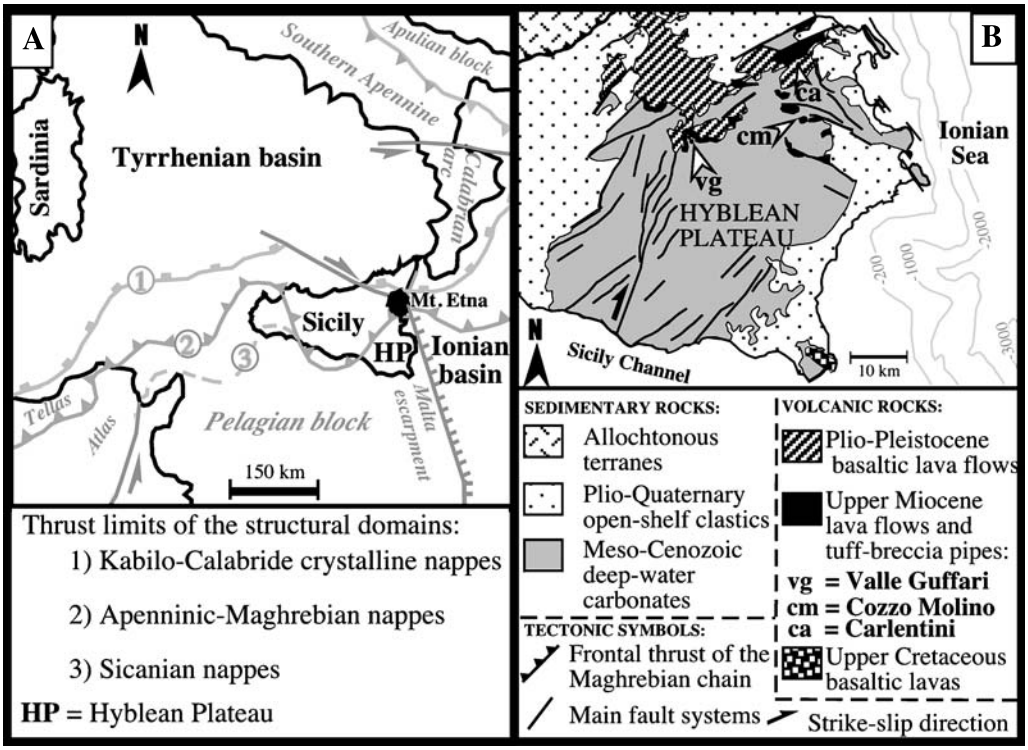

Fig. 1. **A** Main structural domains of Sicily and neighbouring areas (simplified after *Lentini* et al., 1996); **B** Geological sketch map of the Hyblean area and location of the main xenolith occurrences

surface by ascending basaltic and kimberlitic magmas (*Downes*, 1993; *Rudnick*, 1992).

A large number of lower crustal xenoliths have been recently found in a few diatreme pipes in the Hyblean Plateau, in the south-eastern corner of Sicily (Southern Italy; Fig. 1). The Hyblean lower crust has been traditionally considered to belong to the African continental crust (*Burollet* et al., 1978: *Lentini* et al., 1996; *Catalano* et al., 2000). This conclusion is largely based on the interpretation of seismic data. However, only one seismic line crosses the western margin of the Hyblean Plateau (*Carrozzo* et al., 1987) and a few other refraction and reflection profiles transect only neighbouring areas (*Catalano* et al., 2000). Moreover, the interpretation of seismic soundings is closely related to a chosen lithological model. For instance, experimental results show that partially serpentinized peridotites have seismic wave velocities (V_p, V_s) similar to granitoids and other felsic rocks (e.g. *Hyndman* and *Peacock*, 2003).

Positive Bouguer anomaly and strong magnetic anomalies (up to 4500 cgs) have been interpreted as due to the presence of large mafic igneous masses just below the sedimentary-volcanic Meso-Cenozoic succession (*Arisi Rota* and *Fichera*, 1987; *Ciminale* and *Wasowski*, 1989). According to *Vai* (1994), the distribution of pelagic deposits within the southern Mediterranean area suggests that the Hyblean Plateau may represent the western part of the Permo-Triassic Palaeo-Tethys ocean. Moreover, *Sapienza* and *Scribano* (2000) underlined the absence among the xenoliths of

lithologies typical of the continental middle-upper crust (e.g. granitoids, felsic granulites, schists) and the overall basaltic composition of the xenoliths. The choice of the one hypothesis (continental crust) over the other (oceanic crust) has important geological implications, i.e. on the location of the boundary between the African and European plates, on the nature of the eastern border of the Pelagian block (Fig. 1) and, more generally, on the geodynamic evolution of the Central Mediterranean area.

In this paper we present new whole rock (major and trace elements) and mineral chemistry (major elements) data of a suite of lower crustal xenoliths collected from the Hyblean Plateau, giving major emphasis to the gabbroic lithotypes. We also incorporate published data (*Scribano*, 1988; *Mazzoleni* and *Scribano*, 1994; *Tonarini* et al., 1996; *Punturo*, 1999; *Sapienza* and *Scribano*, 2000; see Table 1). The main aim of this study is to understand the origin and original tectonic setting of the deep Hyblean crust. It is opportune to refer to the case of Pannonian Basin (*Embey-Isztin* et al., 2003) as an example of a study that started with the assumption that the xenoliths were continental in origin, having instead produced the surprising result that that region is underlain by rocks of oceanic derivation.

Geological setting

The island of Sicily is located in the central Mediterranean area, in a geodynamic environment related to the collisional movement between the European and African Plates (*Dewe*y et al., 1989). In the central Mediterranean area, *Lentini* et al. (1996) described three main structural domains (Fig. 1): (a) the *hinterland domain*, i.e. Tyrrhenian Basin and Sardinia-Corsica block; (b) the *orogenic domain* consisting of the Apenninic-Maghrebian thrust system and (c) the *foreland domain*, which represents undeformed crustal sectors not involved in the Apenninic-Maghrebian orogeny, i.e. Pelagian block and Ionian basin. The latter is generally considered to be an undeformed relict of oceanic crust of probable Jurassic age (e.g. *Finetti*, 1982). Recently *Catalano* et al. (2000), interpreting seismic reflection profiles, have distinguished two Ionian crustal sectors: the western, showing transitional-type crust and the eastern, consisting of old oceanic lithosphere.

The Hyblean Plateau is an emergent portion of the Pelagian block. It is in contact with the Gela nappe, belonging to the Apenninic-Maghrebian thrust system (north-western) and the Malta Escarpment (east) which separates the Plateau from the Ionian Basin. The exposed part of the Hyblean sedimentary sequence consists of Upper Cretaceous to Miocene deep-water carbonates and Plio-Quaternary open-shelf clastics, with intercalation of different levels of basic volcanic rocks (*Bianchi* et al., 1987; Fig. 1). Commercial boreholes have reached Triassic carbonates and basic igneous rocks at about 3 km b.s.l., and geophysical data suggest that this entire sequence is 8–10 km thick (*Chironi* et al., 2000). Two main fault systems cross-cut the Hyblean area. One, trending NE–SW, is extensional; the other, trending NNW–SSE, mostly consists of strike-slip faults (*Grasso* and *Reuther*, 1988). Three main magmatic episodes have been recognised: Cretaceous alkali-basalts (*Romano* and *Villari*, 1973), upper Miocene alkali-basalts and tuff-breccia pipes (*Cristofolini* et al., 1981; *Carbone* and *Lentini*, 1981) and Plio-Pleistocene lavas. The Plio-Pleistocene lavas are tholeiitic to alkaline basalts, basanites and rare

nephelinites. They are primary liquids whose different compositions depend on the degree of partial melting, the different depths and the metasomatic enrichments of the source (*Beccaluva* et al., 1998). Interpretation of the Sr–Nd–Pb isotopic data for the Upper Miocene and Plio-Pleistocene lavas has excluded the presence of continental crust contamination (*Trua* et al., 1998; *Bianchini* et al., 1999).

Petrography

Ultramafic and feldspar-bearing xenoliths occur in Miocene pipes of the Hyblean Plateau. The tuff-breccia deposit from Valle Guffari (*vg*; Fig. 1) is the most significant xenolith occurrence in the region. The ultramafic suite consists of mantle-derived material, represented by spinel lherzolites, spinel harzburgites and various pyroxenite types, i.e. Cr-diopside websterites, Al-augite websterites, spinel and garnet clinopyroxenites (*Scribano*, 1987; *Nimis* and *Vannucci*, 1995; *Punturo* et al., 2000).

The feldspar-bearing suite, which is considered to be derived from the Hyblean lower crust, consists of sub-rounded xenoliths 5 to 15 cm in diameter. They lack evident infiltrations of the host basaltic melt. On the basis of texture and mineral association, we have subdivided them into three main groups, whose relative proportions are roughly estimated from the number of collected xenoliths: *i*) mafic granulites, ≈60%, *ii*) gabbros, ≈30%, and *iii*) diorites, ≈10%. Both gabbros and diorites show different degrees of shearing, recrystallization and metasomatic transformations. The gabbros are the subject of this study.

Gabbros

Plagioclase, clinopyroxene, Fe–Ti oxides, green hercynitic spinel, apatite and rare red-brown amphibole form the gabbro paragenesis. These still preserve their igneous texture in spite of having undergone shearing and more or less pronounced metamorphic re-equilibration.

Ductile and brittle deformation textures are widespread in these xenoliths. The plagioclase porphyroclasts (Pl I) show either crystal-plastic deformation or notable grain-size reduction due to recrystallisation (plagioclase neoblasts: Pl II; Fig. 2a,b). Conversely, most of the pyroxenes show brittle deformation (clinopyroxene

Fig. 2. Textural features of xenoliths from Hyblean diatremes. **a** relic plagioclase porphyroclast (Pl I) within the matrix formed by re-crystallised clinopyroxene (Cpx II) and plagioclase (Pl II) in oxide-rich gabbros (crossed nicols); **b** grain-size reduction along shear plane between porphyroclasts in oxide-rich gabbros (plane light); **c** anhedral Fe–Ti oxides III related to glassy pockets within the oxide-rich gabbro matrix; deformed sub-rounded Cpx I is visible (plane light); **d** sheared texture in oxide-rich gabbro (plane light). Plagioclase appears white, clinopyroxene grey, Fe–Ti-rich oxide (III) black; **e** corrosion edge in plagioclase porphyroclasts (Pl I) in contact with glassy pockets (plane light); **f** scanned polished surface of a sheared diorite xenolith FB-h3; **g** polished surface of diorite xenolith FB-h2 showing modal layering and brittle fractures. Mineral whitish to pale grey is plagioclase, medium-grey is pyroxene. Full explanation is given in the text; **h** granoblastic texture in mafic granulite (plane light)

porphyroclasts: Cpx I) rarely surrounded by pyroxene neoblasts (Cpx II) (Fig. 2b, c, d). Cpx I shows abundant ilmenite exsolution lamellae, while Cpx II is exsolution-free (Fig. 2c).

Fe–Ti oxides occur included in silicates (Fe–Ti oxides I; Fig. 2b), as scattered grains (2–5 vol%; Fe–Ti oxides II) interstitial to silicates or, most commonly, as anhedral amoeboid-shaped grains, forming large opaque patches (8–18 vol%;

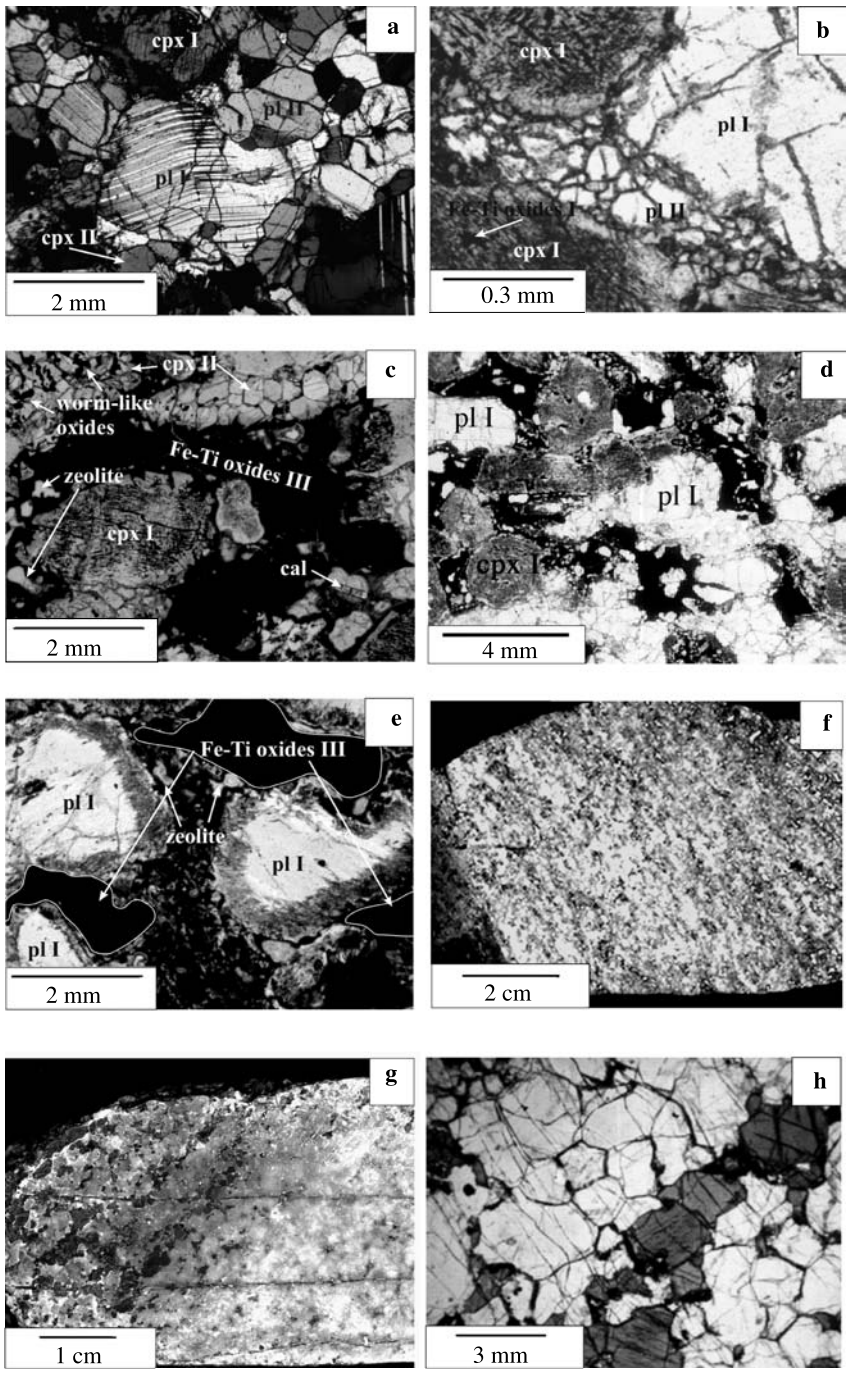

Fe–Ti oxides III) within the grain frame of the gabbro (Fig. 2c, d, e). Locally, anhedral micrograins of green hercynitic spinel are found within these patches. On the basis of the Fe–Ti oxide modal abundances, the gabbros can be subdivided into two subgroups: the oxide-rich gabbros (Fe–Ti oxides ≥ 8 vol%) and oxide-poor gabbros (Fe–Ti oxides ≤ 8 vol%).

The Fe–Ti oxides III are generally associated with melt pockets. These pockets of altered, turbid silicate glass with fine-grained clinopyroxene, plagioclase and opaque ores are ubiquitous and especially abundant in the oxide-rich gabbros. They show disequilibrium relationships with the neighbouring silicates: Pl I grains in contact with the glass are strongly corroded (Fig. 2e), while Cpx I grains exhibit a thin purplish rim (Fig. 2c). Zeolites fill vugs occuring in these pockets. The volume of melt pockets, and thus Fe–Ti oxide III, is positively correlated with the degree of deformation of the host rocks. A number of secondary minerals (i.e. Fe–Mg amphiboles, chlorites, smectites, Na-rich zeolites, calcite and Fe-hydroxides; Fig. 2c, e) fill both vugs and veinlets or locally replace primary minerals.

Diorites

Diorites are coarse- to medium-grained leucocratic rocks. Their paragenesis is dominated by Na-rich plagioclase with subordinate clinopyroxene and Fe–Ti oxides. They show variable microstructures.

The most common type shows an evident lineation (Fig. 2f) due to the alignment of finely granulated pyroxene relics in a matrix of medium- to fine-grained feldspar crystals. Locally, a double shell of Fe–Ti hydroxides (outer shell) and calcite (inner shell) separates the pyroxene grains from the feldspar matrix. In some cases aggregates of polycrystalline calcite replace the pyroxene. A slightly pleochroic bronzite occurs in these rocks, up to 6 vol%, either as anhedral isolated grains or tiny, corroded relics surrounded by calcite.

Another type of diorite, coarser grained than the first variety and partially recrystallized, shows modal layering due to alternating 3–5 cm thick layers rich in feldspar and thinner, darker layers rich in pyroxene and opaques. Pyroxene grains are often rimmed and locally replaced by a yellowish turbid material consisting of fine aggregates of secondary minerals hosting tiny vugs filled with analcite and zeolites. The same material also fills brittle micro-fractures occurring in the rock as subparallel sets discordant to the layering (Fig. 2g).

Plagioclase from the diorite xenoliths is affected by different degrees of alkaline metasomatism in the form of albite and (subordinate) K-feldspar veins (*Scribano* et al., 2003). In addition, chlorites, zeolites, smectites, Fe-oxide/hydroxides and carbonates are ubiquitous in these rocks, partially replacing the igneous minerals.

In a few cases, the metasomatic transformations and deformations have totally obliterated the original mineral compositions and textures. Fractured relics of alkali feldspar (An_3–Ab_{80}–Or_{17}), surrounded by tiny rounded or elongated feldspar neoblasts, are embedded in an abundant matrix of chlorites and smectite. Rare irregular hematite grains and a number of tiny opaque patches also occur in the phyllosilicate matrix. The alkali feldspar porphyroclasts exhibit chessboard extinction, 82–85% triclinicity and a low-temperature structural state (*Scribano* et al., 2003). In one of these metasomatic rocks (sample FBZ) several monazite

and zircon grains have been found in the chlorite patches. These metasomatic rocks closely resemble the hydrothermal zircon-bearing, alkali feldspar – chlorite ''blackwalls'', enveloping rodingite bodies from ophiolite massifs (e.g. Sudetic ophiolite, SW Poland: *Dubinska* et al., 2004). A detailed mineralogic and geochemical study on these metasomatic rocks will be reported elsewhere, though the preliminary results supplied by *Scribano* et al. (2003) will be taken into account for the present discussion.

Mafic granulites

Scribano (1988) gave a preliminary report on the petrography of the mafic granulites. The following summarises their principal features. Hyblean granulites show granoblastic microstructures with fine (0.3–1 mm) to medium (0.5–3 mm) grain sizes (Fig. 2h). They consist of plagioclase, clinopyroxene, orthopyroxene and green Al-spinel. Generally, clusters of pyroxenes and plagioclase grains are randomly distributed in the rocks. Rarely, mafic and felsic minerals are arranged in alternating irregular layers visible at the hand-specimen scale. The occurrence of rare spinel-bearing anorthositic granulites and even rarer feldspar-bearing pyroxenites have also been reported. Fine exsolution lamellae of Ca-poor from Ca-rich pyroxene and vice-versa are common in the pyroxenes. Spinel occurs as worm-shaped intergrowths in the pyroxene grains, as discrete grains between the coexisting silicates and more rarely as ''droplets'' enclosed in the feldspars. Striking coronitic textures and trails of CO_2 fluid inclusions are common in these rocks (*Scribano*, 1988; *Pompilio* and *Scribano*, 1992).

Analytical techniques

Table 1 reports the sample set considered. To supplement the existing data on the mafic granulites, representative samples of oxide-rich and oxide-poor gabbros and diorites were selected. Chemical analyses of minerals were performed at the C.N.R. Instituto di Geoscienze e Georisore (I.G.G.), Padova, using a Cameca Camebax equipped with four wavelength-dispersive spectrometers. Operating conditions were 15 kV and 15 nA. Synthetic oxides and minerals were used as standards. X-ray intensities were automatically corrected to oxide percent concentrations by on-line PAP procedure. Additional analyses were performed using a Cambridge Instrument SEM fitted with an EDS Link (operating conditions: 1.5 kV, 20 nA, lifetime 100 s, ZAF corrections) at the Istituto Nazionale di Geofisica e Vulcanologia – Catania.

Geochemical analyses were performed at Service d'Analyse des Roches et des Minéraux (SARM) laboratories in Nancy, France. Whole-rock major elements were obtained by Inductively Coupled Plasma Emission Spectrometry (ICP), trace elements by Inductively Coupled Plasma Mass Spectrometry (ICP-MS). CO_2 was detected volumetrically. Total iron is reported as Fe_2O_3. Detailed information on analytical methods and detection limits are reported in: www.crpg.cnrs.nancy.fr/SARM.

The whole rock $\delta\ ^{18}O$ values have been obtained at Activation Laboratories (Ancaster, Ontario). Oxygen was extracted from powders of whole rocks by

Table 1. *Summary of Hyblean lower crustal samples included in this study, references and provenance sites.* Vg *Valle Guffari;* Cm *Cozzo Molino (see Fig. 1).* cpx *clinopyroxene;* pl *plagioclase;* ox *Fe–Ti oxides;* spl *Al-spinel*

Sample	Data	Ref*	Area
Ia) Oxide-rich gabbros			
XLP1	Major, trace, REE elements, cpx, ox and pl compositions	1	Vg
FB-f4	Major, trace, REE elements, cpx, ox and pl compositions	1, 2	Vg
FB80	Major, trace, REE elements, cpx, ox and pl compositions	1	Vg
FB-f31	Major, trace, REE elements, cpx, ox and pl compositions	1, 2	Vg
FB50	Major, trace, REE elements, cpx, ox and pl compositions	1	Vg
VB5	Major, trace, REE elements, cpx, ox and pl compositions	1	Vg
ML17	Major, trace, REE elements	3	Vg
FB-f1	Major, trace, REE elements, cpx, ox and pl compositions	1, 2	Vg
Ib) Oxide-poor gabbros			
FB70	Major, trace, REE elements, cpx, ox and pl compositions	1	Vg
FB-f7	Major, trace, REE elements, cpx, ox and pl compositions	1, 2	Vg
FB13	Major, trace, REE elements, cpx, ox and pl compositions	1	Vg
FBf32	Major, trace, REE elements	1	Vg
FB11	Major, trace, REE elements, cpx, ox and pl compositions	1	Vg
FBe11	Major, trace, REE elements	1	Vg
II) Diorites			
FB12	Major, trace, REE elements, cpx, ox and pl compositions	1	Vg
FB8	Major, trace, REE elements, cpx, ox and pl compositions	1	Vg
FB-h2	Major, trace, REE elements, cpx, ox and pl compositions	1, 2	Vg
FB-h3	Major, trace, REE elements, cpx, ox and pl compositions	1, 2	Vg
FBY	Major, trace, REE elements	1	Vg
III) Mafic granulites			
MVG1	Major, trace, REE elements; cpx, spl and pl compositions	4, 5	Cm
MVG2	Major, trace, REE elements; cpx, spl and pl compositions	4, 5	Cm
MG3	Major, trace, REE elements; cpx, spl and pl compositions	4, 5	Cm
MG4	Major, trace, REE elements; cpx, spl and pl compositions	5, 6	Cm
MG7	Major, trace, REE elements; cpx, spl and pl compositions	5, 6	Cm

* 1: this study; 2: *Sapienza* and *Scribano* (2000); 3: *Punturo* (1999); 4: *Tonarini* et al. (1996); 5: *Scribano* (1988); 6: *Mazzoleni* and *Scribano* (1994)

reaction with BrF_5, converted to CO_2 in a graphite furnace and analysed by mass spectrometer. The isotopic composition of a sample is given as: $\delta_{sample} = (R_{sample}/R_{standard} - 1)^* 1000$ in per milunit, where R is $^{18}O/^{16}O$ and the standard is SMOW.

Mineral compositions

Pyroxenes

Compositions of representative clinopyroxenes are reported in Table 2. Clinopyroxenes from the studied xenoliths are mostly diopsides and only those from sample

Table 2. *Chemical composition of pyroxenes of Hyblean xenoliths. Mg# = Mg/(Mg + Fe^{2+} + Fe^{3+})*100*

	Oxide-rich gabbros		Oxide-poor gabbros			Diorite			
Sample	FB80 P	FB50 P	FB11 N	FB13 N	FB70 N	FB8 N	FB12 N	FB3 N	FB3 N
Wt%									
SiO_2	51.86	50.65	47.49	50.85	50.40	51.25	52.17	52.53	53.60
TiO_2	0.47	0.78	1.87	0.58	0.98	0.49	0.46	0.27	0.00
Al_2O_3	3.47	4.27	7.80	4.07	5.04	3.30	2.57	2.11	0.71
Cr_2O_3	0.03	0.00	0.12	0.00	0.02	0.02	0.03	0.00	0.00
FeO	7.03	7.46	6.82	8.05	8.13	8.72	10.05	9.64	23.0.9
MnO	0.32	0.26	0.19	0.23	0.27	0.53	0.75	0.62	1.15
MgO	13.92	13.61	11.95	13.36	13.18	12.55	13.42	12.61	20.12
CaO	22.79	23.07	22.86	22.98	20.86	21.96	19.24	20.75	0.91
Na_2O	0.46	0.68	0.97	0.67	1.05	1.08	1.27	1.12	0.00
Total	100.35	100.78	100.05	100.79	99.93	99.90	99.96	99.65	99.58
Mg#	78	76	75	77	74	72	70	70	60

FB12 (diorite) are augites. Overall, their Mg# value ranges from 70 to 85. Clinopyroxenes from the mafic granulites show the widest ranges in Mg# (71–85), Al_2O_3 (3.5–9 wt%), TiO_2 (0.5–1.5 wt%) and Na_2O (0.7–1.5 wt%). No intra-granular variations were found in these clinopyroxenes.

Clinopyroxenes from the oxide-rich gabbros show a relatively narrow range of Mg# (73–78; Fig. 3). The cores of the Cpx I generally display Al_2O_3 ~4 wt%, TiO_2 ~0.7 wt% and Na_2O ~0.6 wt%, while their outermost rims in contact with the

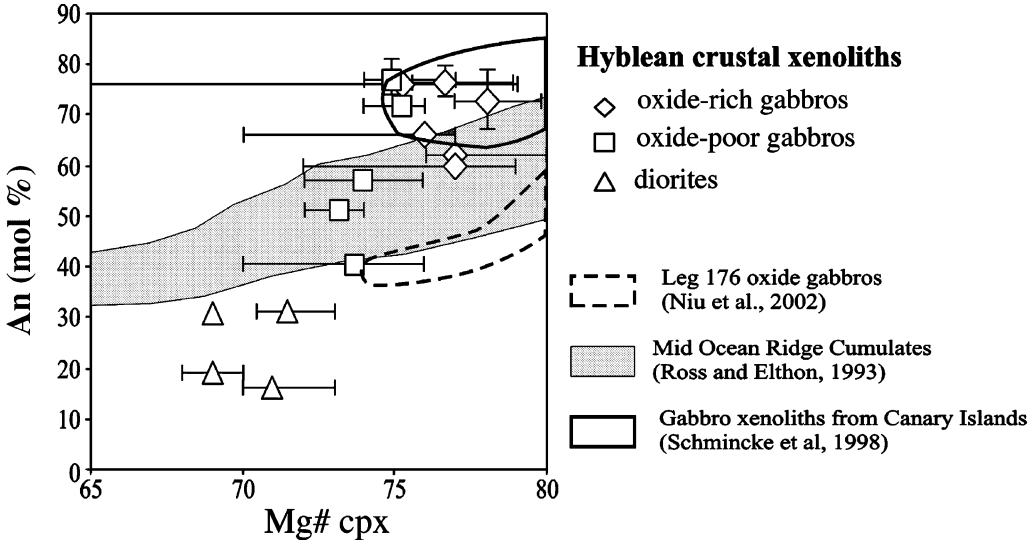

Fig. 3. An (mol%) of plagioclase *vs* Mg# of coexisting clinopyroxenes from the Hyblean gabbros and diorites. The symbols correspond to the average An of plagioclases and Mg# of coexisting clinopyroxenes per sample. The bars indicate the variations within each sample

glassy patches have higher Al_2O_3 and TiO_2 contents. The diorite clinopyroxenes have the lowest average Mg# (69–71; Fig. 3) and show some variations in Al_2O_3 (2–4 wt%), TiO_2 (0.4–0.7 wt%) and Na_2O (1–1.5 wt%). The average Mg# of clinopyroxenes (Cpx II) from oxide-poor gabbros (Mg# = 74–75; Fig. 3) is intermediate between those of oxide-rich gabbros and diorite clinopyroxenes and partially overlaps the former group. Scarce Ca-poor pyroxene (Mg# = 60; CaO ≈90 wt%), coexisting with a calcic one (Mg# = 70; CaO ≈21 wt%), has been found only in recrystallized diorites (e.g. FB-h3: Table 1). Orthopyroxene from mafic granulites shows Mg# = 65–68, 2.0–6.5 Al_2O_3 wt% and 0.2–0.7 CaO wt% (*Scribano*, 1988).

Feldspars

Feldspar compositions in gabbros and diorites are reported in Table 3. Generally, they are plagioclase varying from An_{55} to An_{80} in gabbro xenoliths (except in FB70 which is An_{40}; Fig. 3), from An_{15} to An_{30} in diorites, and from An_{55} to An_{82} in mafic granulites. Plagioclase compositions are something homogeneous within each sample (Fig. 3). The Or content is negligible in gabbro and mafic granulite feldspars, whereas it varies from 2 to 10 mol% in those from diorites.

Oxides

The chemical compositions of representative oxides are reported in Table 4. Opaques included in clinopyroxene and plagioclase porphyroclasts (type I) are Ti-magnetite and ilmenite, while the interstitial oxides (type II) are ilmenite.

Table 3. *Chemical composition of plagioclases of Hyblean xenoliths.* P *porphyroclast;* N *neoblast*

	Oxide-rich gabbro		Oxide-poor gabbro					Diorite	
Sample	FB80 P core	FB50 P rim	FB11 N	FB70 P core	FB70 P rim	FB13 P core	FB13 P rim	FB12 N	FB8 N
Wt%									
SiO_2	50.11	51.08	49.85	57.99	58.32	47.34	49.48	64.64	60.04
TiO_2	0.02	0.00	0.01	0.03	0.02	0.02	0.01	0.02	0.01
Al_2O_3	31.50	30.93	31.51	26.03	26.41	32.68	32.13	21.85	24.43
Cr_2O_3	0.05	0.00	0.00	0.00	0.02	0.00	0.07	0.00	0.00
FeO	0.06	0.13	0.02	0.03	0.05	0.17	0.08	0.04	0.07
MnO	0.01	0.00	0.00	0.00	0.01	0.00	0.06	0.00	0.00
MgO	0.00	0.01	0.01	0.01	0.00	0.00	0.00	0.00	0.02
CaO	14.95	14.18	15.06	8.38	8.56	17.07	15.83	3.17	6.59
Na_2O	3.19	3.81	3.14	6.65	6.79	2.12	2.95	9.06	7.66
K_2O	0.03	0.05	0.05	0.29	0.27	0.02	0.07	1.56	0.47
BaO	0.000	0.000	0.10	0.00	0.02	0.00	0.16	0.00	0.10
Total	99.91	100.20	99.75	99.41	100.48	99.42	100.84	100.34	99.39
Ab mol%	27.9	32.8	27.1	58.3	58.2	18	25.3	76.8	66.3
An mol%	71.9	66.9	72.6	40.1	40.3	81.9	74.3	14.6	31
Or mol%	0.2	0.3	0.3	1.6	1.5	0.1	0.4	8.6	2.7

Table 4. *Chemical composition of Fe–Ti oxides of Hyblean xenoliths. Types (I, II, III) are explained in the text*

	Oxide-rich gabbro					Oxide-poor gabbro		Diorite	
Sample	FB80	FB80	FB80	FB4	FB4	FB7	FB70	FB13	FB13
Type	I	III	III	III	III	II	I	III	I
Wt%									
SiO_2	0.08	0.03	0.03	0.08	0.06	0.06	0.00	0.00	0.00
TiO_2	7.93	52.11	0.05	53.89	19.23	10.36	43.45	38.99	41.43
Al_2O_3	2.71	0.60	60.03	0.33	6.26	3.84	0.84	0.28	0.77
FeO	80.98	39.31	24.57	35.70	63.65	77.78	50.66	55.06	54.46
MnO	0.34	0.61	0.27	0.77	0.58	0.34	0.43	0.48	0.38
MgO	2.82	6.68	11.83	8.50	6.96	1.96	3.15	2.69	1.34
CaO	0.04	0.08	0.00	0.07	0.08	0.00	0.04	0.00	0.05
Cr_2O_3	0.06	0.00	0.11	0.03	0.01	0.34	0.05	0.00	0.00
Total	94.96	99.42	96.89	99.37	96.83	94.68	98.63	97.50	98.43

The patch-forming oxides (type III), characteristic of, but not restricted to the oxide-rich gabbros, consist of a coarse intergrowth of ilmenite and Ti-magnetite and rare green hercynitic spinel (FeO ∼24 wt%; Al_2O_3 ∼60 wt%). Spinel from the mafic granulites displays Al_2O_3 content from 46 to 65 wt%, FeO from 15 to 39 wt%, MgO from 10 to 17.5 wt%. Cr_2O_3 content never exceeds 6.5 wt% (*Scribano*, 1988).

Amphiboles

Amphibole in the oxide-poor gabbro FB70 is a titanian pargasite (*Leake* et al., 1997) with Mg# = 63. TiO_2, Al_2O_3 and CaO contents are 3.7 wt%, 13.4 wt% and 11.7 wt%, respectively (Table 5). In the glassy pockets within the gabbro and diorite xenoliths,

Table 5. *Chemical composition of amphibole of Hyblean oxide-poor gabbro FB70*

Sample	FB70 core	FB70 rim
Wt%		
SiO_2	40.45	40.56
TiO_2	4.37	3.70
Al_2O_3	13.34	13.40
Cr_2O_3	0.00	0.01
FeO	12.66	12.42
MnO	0.17	0.29
MgO	11.51	11.82
CaO	11.40	11.69
Na_2O	2.96	2.95
K_2O	0.92	0.91
Total	97.77	97.74

SEM investigations showed the presence of actinolite ($Al_2O_3 = 0.9$ wt%; CaO = 10 wt%; Mg# = 60). Rare pargasite also occurs in the mafic granulites (Mg# = 80; $TiO_2 = 2.7$ wt%; $Al_2O_3 = 16.5$ wt.%, CaO = 11.4 wt%; *Scribano*, 1988).

Whole-rock chemistry

New major and trace element data of Hyblean lower crustal xenoliths are reported in Table 6. The following discussion of the data refers to the entire sample set (Table 1). The whole rock composition of the host alkali-basalt (sample LOR) is also reported for comparison.

Major elements

Figure 4 shows the major element variations against MgO content of the Hyblean lower crustal xenoliths. The bulk composition of the gabbros is strongly mode-dependent: they show the widest variations in SiO_2 (from 36.4 to 49.6), Fe_2O_3 (from 11.5 to 22.7 wt%) and TiO_2 (from 2.9 to 5.5 wt%), driven by the modal abundance of Fe–Ti oxides.

The diorite xenoliths show the highest SiO_2 (up to 57 wt%) and alkali contents ($Na_2O = 5.5$–7.3 wt% and K_2O up to 2.5 wt%; always $Na_2O > K_2O$). This composition is related to the modal abundance of Na-plagioclase, which has been affected by pervasive alkaline metasomatism. Diorites also show low MgO and CaO contents. The gabbros and the mafic granulites have $K_2O \leq 0.2$ wt%, with the latter showing the lowest K_2O contents (0.04–0.09 wt.%). P_2O_5 is always < 1 wt.% in all xenoliths, except for the apatite-rich oxide-rich gabbro ML17 (3.5 wt.%). The loss on ignition (LOI) in gabbros and diorites (1.9–6.2 wt.%) is higher than in mafic granulites (1.5–0.7 wt.%). CO_2 contents never exceed 0.5 wt%, except in some diorites whose clinopyroxene grains are partially replaced by calcite (e.g. 3.6 wt% in sample FB-h3).

Trace elements

Figure 5 shows chondrite-normalised Rare Earth Element (REE) patterns and N-MORB normalised spiderdiagrams of the Hyblean lower crustal xenoliths. The REE patterns of all gabbro xenoliths are flat from La to Sm or slightly LREE enriched ($La_N/Sm_N \sim 0.7$–1.7). They generally show a moderate positive Eu anomaly ($1 \leq Eu/Eu^* \leq 2$, where $Eu^* = (Sm_N + Gd_N)/2$; *Salters* and *Shimizu*, 1988). MREE are fractionated with respect to the HREE. Samples VB5 and Fbe11 show a similar pattern as the other gabbros except for the Eu anomaly. The pyroxene-rich and oxide-rich gabbro FB-f1 shows an upward-convex REE pattern with LREE depletion ($La_N/Sm_N \sim 0.5$).

The diorite xenoliths show a marked LREE/HREE fractionation ($La_N/Yb_N = 8.5$–20.4) with a pronounced positive Eu anomaly (Eu/Eu^* up to 4.7), indicating that accumulation of plagioclase played an important role in the diorite formation. The mafic granulites show the lowest REE abundances, with LREE/HREE fractionation ($La_N/Yb_N = 1.5$–4.5). A positive Eu anomaly is also present.

In the N-MORB-normalised incompatible elements diagrams (Fig. 5), the gabbros and diorites are generally enriched from Rb to P, with evident Ba and Sr

Table 6. *Major and trace element composition of Hyblean lower crustal xenoliths.* n.a. *not analysed;* b.d.l. *below detection limit*

	Oxide-rich gabbros					Oxide-poor gabbro				Diorites			Host lava
	XLP1	FB50	FB80	VB5	FBf32	FB13	FB11	FBe11	FB70	FB8	FBY	FB12	LOR
(wt%)													
SiO_2	39.51	39.08	39.83	42.68	45.66	43.08	46.76	48.4	46.01	51.99	48.51	56.73	41.56
TiO_2	4.73	4.03	3.8	2.89	2.23	2.41	0.96	1.26	2.19	1.43	2.49	1.52	2.29
Al_2O_3	12.9	14.85	15.55	10.75	20.39	21.58	22.07	13.66	15.76	19.99	15.83	18.36	12.35
$Fe_2O_{3\ tot}$	16.97	15.22	14.90	12.75	6.48	9.9	4.57	9.93	10.01	5.40	9.27	5.01	10.78
MnO	0.17	0.14	0.15	0.15	0.07	0.07	0.06	0.12	0.14	0.06	0.19	0.09	0.15
MgO	6.73	7.43	7.28	9.77	5.3	4.27	5.71	9.14	6.64	3.61	3.61	2.67	11.61
CaO	12.47	13.82	13.4	16.29	13.35	13.37	16.17	12.29	11.89	6.35	8.17	4.23	9.83
Na_2O	2.23	1.59	1.23	1.66	2.5	2.37	2.03	2.44	3.01	5.8	5.48	6.03	1.85
K_2O	0.13	0.22	0.16	0.16	0.17	0.12	0.09	0.18	0.23	0.6	1.16	2.46	1.15
P_2O_5	0.36	0.17	0.08	0.34	0.18	0.25	0.12	0.06	0.34	0.11	0.76	0.35	1.15
LOI	3.37	3.58	2.49	2.61	3.72	2.63	1.9	2.41	3.64	4.57	4.6	2.67	7.25
H_2O	n.a.	3.01	2.35	2.36	n.a.	2.49	1.64	n.a.	3.16	4.17	1.28	2.53	n.a.
CO_2	n.a.	0.57	0.14	0.25	n.a.	0.14	0.26	n.a.	0.48	0.4	3.32	0.14	n.a.
tot	99.57	100.13	98.87	100.05	100.05	100.05	100.44	99.89	99.86	99.91	100.07	100.12	99.97
$Mg^{\#}$	*48.02*	*53.22*	*53.23*	*64.1*	*65.58*	*50.14*	*74.44*	*68.18*	*60.70*	*60.89*	*47.57*	*55.37*	*70.75*
La (ppm)	8.34	6.03	6.79	9	5.04	7.21	3.7	4.08	17.12	7.54	38.93	20.66	81.45
Ce	22.84	14.83	16.19	23.34	13.29	15.38	9.52	11.4	39.78	14.22	85.06	44.14	151.91
Pr	3.52	2.22	2.48	3.63	1.86	2.08	1.55	1.73	5.33	1.7	11.31	5.89	16.41
Nd	18.34	11.57	12.38	18.86	9.39	10.17	8.64	9.4	24.49	7.36	49.42	26.45	60.69
Sm	4.84	3.02	3.49	5.26	2.4	2.37	2.39	3.26	5.32	1.8	10.25	5.7	11
Eu	2.11	1.37	1.48	2.01	1.36	1.17	1.14	1.32	2.39	1.28	5.17	4.34	3.36
Gd	4.75	3.15	3.48	5.31	2.33	2.25	2.46	3.92	4.91	1.62	8.47	4.86	9.77
Tb	0.66	0.44	0.49	0.73	0.32	0.31	0.31	0.6	0.7	0.24	1.1	0.65	1.2
Dy	3.56	2.32	2.66	4.07	1.74	1.65	1.72	3.51	3.79	1.33	5.59	3.44	6.22

(*continued*)

Table 6 (*continued*)

	Oxide-rich gabbros					Oxide-poor gabbro				Diorites			Host lava
	XLP1	FB50	FB80	VB5	FBf32	FB13	FB11	FBe11	FB70	FB8	FBY	FB12	LOR
Ho	0.58	0.4	0.48	0.69	0.3	0.27	0.29	0.58	0.66	0.24	0.93	0.57	1.06
Er	1.37	0.96	1.07	1.65	0.71	0.63	0.68	1.45	1.75	0.59	2.24	1.33	2.54
Tm	0.16	0.12	0.14	0.21	0.09	0.08	0.09	0.19	0.22	0.09	0.26	0.16	0.33
Yb	0.97	0.73	0.84	1.28	0.56	0.48	0.48	1.14	1.31	0.49	1.49	0.91	1.92
Lu	0.15	0.11	0.12	0.18	0.08	0.07	0.07	0.16	0.2	0.06	0.2	0.13	0.29
Rb	14	10	4.9	13	5.3	5.6	3.2	6.8	3.8	19	9.1	9.3	19
Ba	331	247	131	1222	202	168	105	115	323	472	2085	2546	560
Th	0.21	0.2	0.25	0.41	b.d.l.	0.23	0.07	0.41	0.29	0.38	0.39	b.d.l.	8.6
U	0.1	0.07	0.09	0.16	b.d.l.	0.1	b.d.l.	0.12	0.09	0.13	0.38	b.d.l.	2.6
Nb	6.1	5.3	6.2	5	5.2	4	0.69	3.9	12	6.7	23	9.3	88
Ta	0.58	0.49	0.52	0.44	0.58	0.37	0.07	0.29	0.91	0.55	1.7	0.58	5.3
Sr	1435	3185	1641	636	2718	2569	1541	833	1418	1015	920	910	995
Hf	1.4	1.4	1.6	2.2	0.85	1.1	0.71	1.6	2.2	1.1	0.67	0.3	5.5
Zr	37	40	47	62	25	34	18	47	68	36	25	8.7	268
Y	15	11	12	18	7.4	7.4	7.8	16	18	6.2	24	15	29
V	538	450	436	400	160	308	120	225	256	69	155	48	166
Cr	9.9	38	38	27	80	25	231	127	153	17	11	b.d.l.	353
Co	52	49	48	41	23	32	23	53	35	14	11	5.9	43
Ni	136	120	99	41	21	17	79	132	55	31	36	11	302

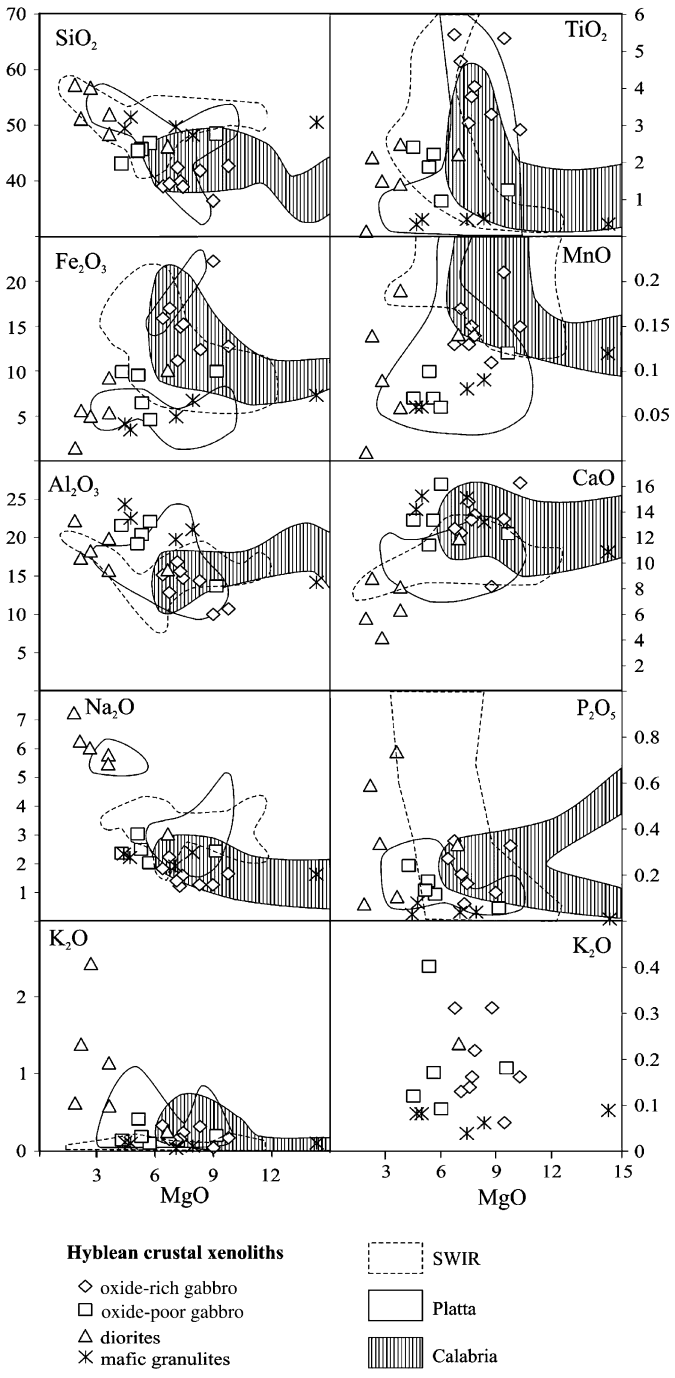

Fig. 4. Whole rock MgO *vs* major oxides for the Hyblean crustal xenolith. For comparison, the fields of gabbroids from different geodynamic settings are also shown

positive anomalies, and depleted in Zr–Hf and HREE. Oxide-rich gabbros patterns are characterised by positive Ti anomaly, in agreement with the relative high modal abundances of Fe–Ti-oxides. Mafic granulites show incompatible element patterns resembling those of the gabbros and diorites but a lower abundance and with a less marked Zr and Hf depletion.

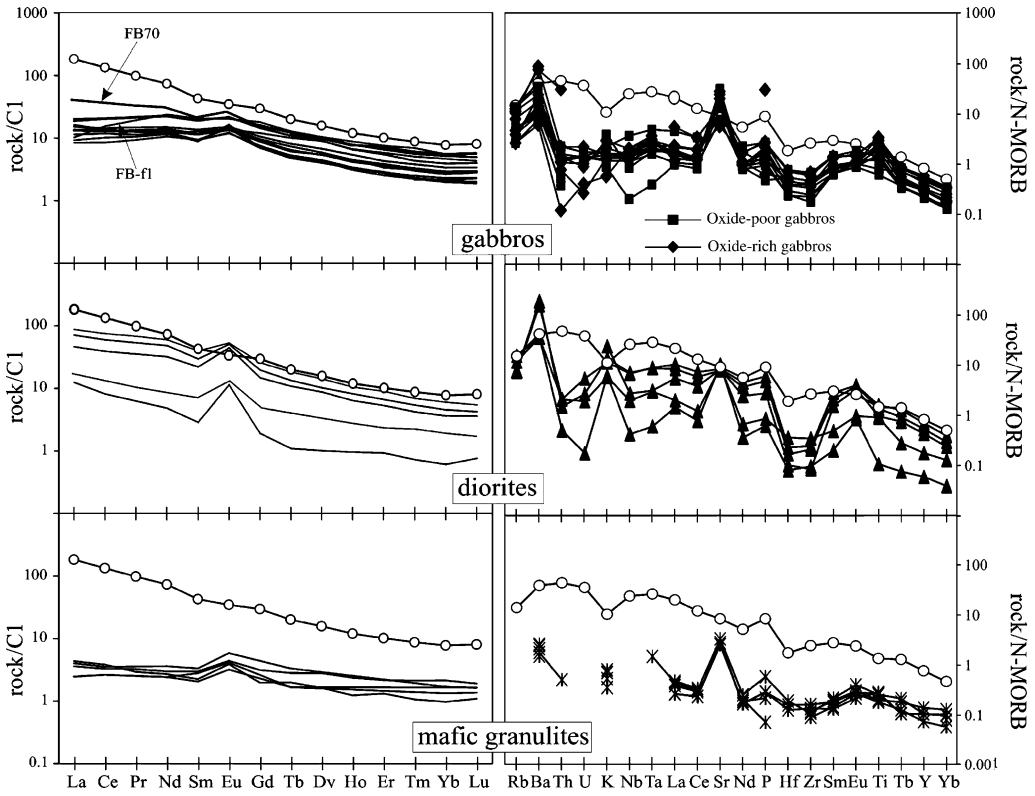

Fig. 5. C1-normalized REE patterns (normalising values after *Anders* and *Grevesse*, 1989) and spiderdiagrams (N-MORB normalising values after *Hoffmann*, 1988; P after *Sun*, 1980) for the Hyblean crustal xenoliths. Open circle: host basalt

Oxygen isotopes

Two samples with no petrographic evidence of important alteration products of primary minerals were chosen for whole rock oxygen isotope analyses. The diorite FB12 has $\delta^{18}O_{SMOW} = 8.7‰$ (LOI = 2.67 wt.%, MgO = 2.67 wt%), and the oxide-poor gabbro FB11 has $\delta^{18}O_{SMOW} = 7.2‰$ (LOI = 1.9 wt%, MgO = 5.71 wt%).

Discussion

Origin of the different groups of Hyblean mafic xenoliths

The textural, mineralogical and geochemical heterogeneity observed in the Hyblean xenoliths suggests that the lower crust beneath south-eastern Sicily has experienced a complex petrological evolution. Petrographic data demonstrate the igneous origin of the gabbros. Their mode-controlled chemical compositions suggest that they represent cumulates. In fact, all studied rocks plot outside the primary basaltic liquids field in Mg# vs SiO_2/Al_2O_3 diagram (Fig. 6).

The term ''cumulate'' is here unrelated to any specific petrogenetic models, i.e. those invoking crystal settling in a large magmatic body (for reviews see *Cawthorn*, 1996). The evident relationship between Fe–Ti oxides III and melt

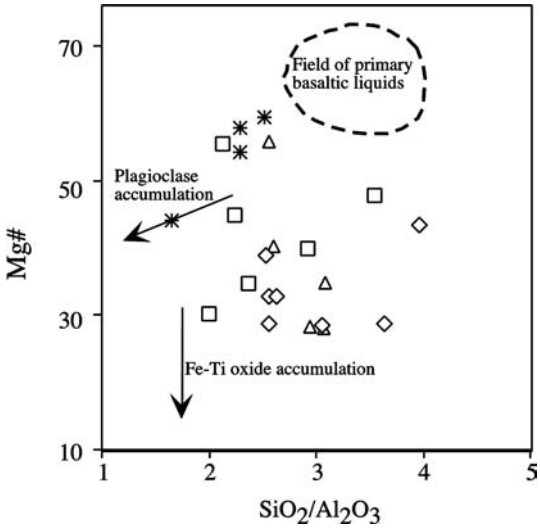

Fig. 6. (SiO_2/Al_2O_3) vs Mg# bivariate plots of Hyblean crustal xenoliths. Field of primary basaltic liquids and directions of mineral phase accumulation after *Kempton* et al. (1995). Same symbols as in Fig. 4

pockets (now glass or devitrified glass), the occurrence in primary phases of reaction rims and embayed microstructures against the melt pockets, and their clear connection with deformation textures, all imply the injection of strongly fractionated Fe–Ti-rich melts, probably filter-pressed from gabbroic or dioritic crystal-mushes, within neighbouring gabbroic cumulate masses under shearing conditions. These melts reacted with the host mineral assemblage and precipitated the large oxide minerals. The Fenner-type fractionation trend leading to the oxide-related melts suggests a tholeiitic nature for their parent magma.

Such magmatic infiltration has been documented in lower crustal xenoliths of the Cima volcanic field by *Wilshire* and *McGuire* (1996), as well as in the oceanic crust of ODP Leg 176 (*Niu* et al., 2002). However, in the first case no massive Fe–Ti oxides are associated with melt pockets, although *Niu* et al. (2002) described them in the gabbros of South West Indian Ridge.

The range of variation of some incompatible element ratios of the gabbro xenoliths (e.g. $Zr/Nb = 5–26$; $Y/Nb = 1.4–11$), and particularly their *average* values ($Zr/Nb = 9$; $Y/Nb = 3$), indicate that these cumulates were derived from MORB-type liquids (*le Roux* et al., 2002). On the other hand these ratios are useless for rocks affected by significant hydrothermal metasomatism, like most of the studied diorites, since Cl–F–CO_2-bearing hydrothermal fluids are capable of mobilizing even those elements that are generally considered highly immobile (e.g. *Vard* and *William-Jones*, 1993; *Geisler* et al., 2002). In fact, the relatively high Nb contents in the diorites FB-h3 and FBY are positively correlated with CO_2 contents, and hence with the occurrence of secondary calcite in these rocks.

The origin of the diorites may be related to fractionation of residual liquids remaining after the formation of some of the cumulate gabbros since calcite-free diorites have Zr/Nb and Y/Nb signatures similar to those of gabbros. However the following additional hypotheses on the origin of diorites cannot be ruled out: (i) some of the Hyblean ''diorites'' may be derived from plagioclase-rich gabbro protoliths which have suffered a strong alkaline metasomatism; (ii) some diorite-related

liquids derive from small degrees of partial melting of gabbros during high temperature shearing (e.g. *Costa* and *Caby*, 2000).

Comparisons of trace element distributions between the xenoliths and the host rock exclude contamination as an important metasomatic agent for Hyblean xenoliths (Fig. 5). For instance, Sr and Ba content in most gabbros, related to plagioclase accumulation, exceeds that of the host rock. However an additional influx of these elements, i.e. interaction with percolating and uprising alkaline silicate melts (e.g. *Neumann* et al., 2000) cannot be excluded.

The positive correlation between LOI and LILE (see Table 6) and the presence of amphibole suggest that the concentration of these elements is also related to processes controlled by late-stage hydrous fluids. Hydrous fluids may also mobilise the alkalis and produce the Na–K-feldspar micro-veinlets cross-cutting the plagioclases of the diorites. Hydrous fluid circulation is in agreement with the relatively high $\delta^{18}O_{SMOW}$ values (FB12 = 8.7‰ and FB11 = 7.2‰). In fact, these values are similar to those of oceanic mafic rocks subjected to various processes including ocean floor weathering (*Staudigel* et al., 1981), but they also fall within the range of granulite xenoliths from deep continental crust (*Kempton* and *Harmon*, 1992).

According to *Scribano* (1988) and *Sapienza* and *Scribano* (2000), mafic granulites are of meta-igneous origin. The chemical compositions of these rocks suggest that they have suffered depletion during granulite-facies recrystallisation. The lack of major element correlation (Fig. 4) among gabbros, diorites and mafic granulites indicates that the latter may not derive from comagmatic protoliths.

Comparisons with gabbroids from different geodynamic settings

In order to define the nature of the Hyblean lower crust and the processes through which it may have evolved, the geochemical and petrographic features of the Hyblean lower crustal xenoliths were compared to igneous (cumulates in most cases) and metamorphic-textured gabbroids from well-known geodynamic settings.

The suite of Hyblean lower crust xenoliths consists of mafic granulites, subordinate gabbros and rare diorites. P–T data from the granoblastic mafic granulites indicates an intermediate pressure of metamorphism, suggesting the existence of a relatively thinned crust. The predominant mineral assemblage (two pyroxenes + plagioclase + Al-spinel) of the Hyblean mafic granulite xenoliths is analogous to that of the European Phanerozoic lower crust, though the latter often bear garnet (*Downes*, 1993). It is possible that the igneous protolith of the mafic granulites was formed by basaltic underplating of continental crust. However, petrographic evidence and geochemistry of the gabbros and diorites argue against a continental origin. Gabbros show shearing microstructures that are related to the melt pockets and Fe–Ti oxides III. Severe shearing and massive oxide patches within a silicate matrix are uncommon in gabbros from continental layered intrusions (*Hunter*, 1996). The continental occurrences of heavily sheared gabbros are rather unique (the Ivrea Verbano Zone, Northern Italy; *Rivalenti* et al., 1984 and *Zingg*, 1990). However, such modal and textural characteristics have been described in oceanic gabbroids, e.g. from transform segments of low-spreading ocean ridges (*Vissers* and *Nicolas*, 1995). These petrographic features are also very common in some ophiolitic ferrogabbros and ferrodiorites, i.e. those from the Italian Northern Apennines

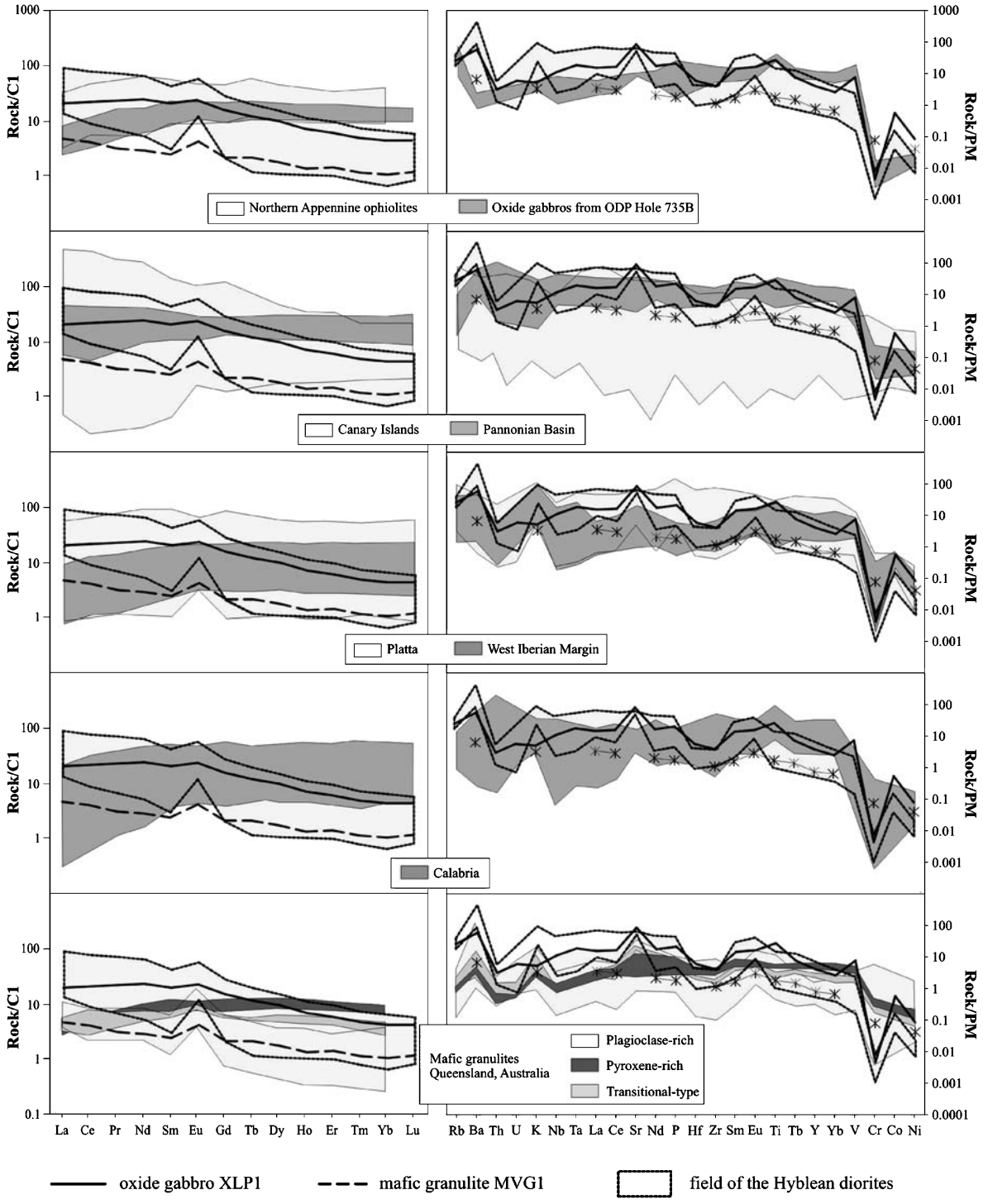

Fig. 7. C1-normalised REE patterns and PM-normalised spiderdiagrams for gabbroids from different geodynamic settings. See text for references. Representative Hyblean xenoliths are reported: black line = average gabbro; dashed line/asterisk = average mafic granulite; field with dotted line = diorites

and Western Alps (*Pognante* et al., 1983; *Tribuzio* et al., 1995, 1999; *Tiepolo* et al., 1997).

Another argument supporting the oceanic affinity of Hyblean gabbros is the covariation between the anorthite content of plagioclase and the Mg# value of coexisting clinopyroxene (Fig. 3). Most data for the Hyblean oxide-rich gabbros is in agreement with the fields defined by oceanic gabbro xenoliths from the Canary Islands (*Schmincke* et al., 1998), while the oxide-poor gabbros fall within the range of Mid Ocean Ridge cumulates (*Ross* and *Elthon*, 1993: Fig. 3).

In Fig. 4, the whole-rock major element composition of the Hyblean gabbros is compared with that of oxide-rich gabbros from the South West Indian Ridge (oceanic crust; *Coogan* et al., 2001), gabbroids from Platta (ocean-continent transition; *Desmurs* et al., 2002) and Calabria (continental; *Morten*, unpublished data). The suite of Hyblean lower crustal xenolithst mostly resembles those of the Platta gabbroic suite (including Mg-, Fe-, Fe–Ti–P-gabbros and diorites) and the oxide-gabbros from South West Indian Ridge.

Figure 7 shows C1-normalized REE patterns and N-MORB-normalized spiderdiagrams for gabbroids (cumulates in some cases) from different geodynamic settings. The enrichment of LREE over HREE is considered typical of the lower continental crust ($La_N/Yb_N > 1$; *Downes*, 1993). Nevertheless some exceptions exist (e.g. metagabbros from Calabria, Pannonian Basin). Conversely, gabbroids with oceanic affinity usually show almost flat or LREE depleted patterns ($La_N/Yb_N < 1$; *Coogan* et al., 2001). The Hyblean diorites show REE patterns and N-MORB-normalised spiderdiagrams similar to the plagioclase-rich mafic granulites from Queensland, although the latter have lower LREE and trace element concentrations. *Rudnick* (1992) interpreted such REE patterns as conforming to those of plagioclase in equilibrium with mafic to intermediate liquids. The N-MORB-normalised trace element distribution of Hyblean gabbros is also comparable to those of the West Iberian Margin (*Cornen* et al., 1999), Pannonian Basin (*Embey-Isztin* et al., 2003) and oxide-rich gabbros from South West Indian Ridge (*Coogan* et al., 2001), with the main differences regarding the Sr and Ba anomalies.

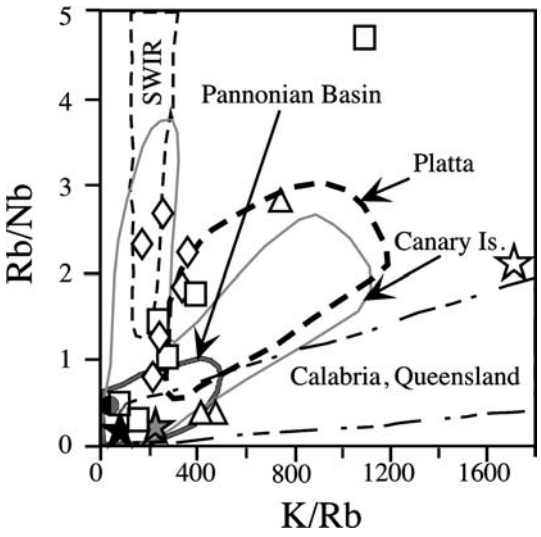

Fig. 8. Relations between Rb/Nb and K/Rb ratios. Same symbols as in Fig. 4. Open star = Lower Continental Crust (*Weaver* and *Tarney*, 1984); black star = LOR (host basalt); grey star = N-MORB (*Hoffmann*, 1988); full circle = P-MORB (*le Roex*, 1987). For comparison, the fields of gabbroids from different geodynamic settings are also shown (see text for references)

The Hyblean lower crustal xenoliths and the gabbroic suites used as comparison are plotted in Fig. 8 (K/Rb *vs* Rb/Nb binary plot). Continental gabbroids exhibit higher K/Rb and lower Rb/Nb ratios than the oceanic and ocean-continent transition gabbroids. The Hyblean xenoliths partially overlap the fields of granulites from the Pannonian Basin and gabbroids from Canary Islands and South West Indian Ridge. Conversely, they lie far from the representative points of continental crustal gabbroids and lower continental crust.

Concluding remarks

The Hyblean xenolith suite consists of upper mantle lithologies, lower-crustal mafic granulites, minor oxide-poor and oxide-rich gabbros, rare diorites, and samples from different levels of the sedimentary sequence at time of the eruption (Upper Miocene). Felsic and garnet-bearing lithotypes are absent from the suite. The petrological and geochemical data discussed above suggest the following conclusions:

1. The Hyblean gabbros are cumulates formed from liquids with MORB affinity. Strongly fractionated Fe–Ti-rich melts of probable intercumulus origin have been filter-pressed and then injected into adjacent gabbroic masses during shearing. These injected liquids precipitated oxide minerals, giving rise to the oxide-rich gabbros.
2. Some gabbros and most diorites show important chemical and mineralogical transformations (i.e. pervasive alkali metasomatism of plagioclase), related to late-stage and hydrothermal fluids which caused LREE and alkali enrichments.
3. Mafic granulite xenoliths are not comagmatic with the other xenolith groups. Hence they are almost unaffected by metasomatism and hydrothermal alteration and probably derived from the lowest section of the crustal column.
4. The petrographic features of studied oxide-rich gabbros closely resemble those of gabbros drilled and recovered in oceanic environments, especially in the fracture zones of slow-spreading ridges.

These petrographic considerations on the crustal xenoliths can be combined with the following evidence: (i) geophysical investigations (*Arisi Rota* and *Fichera*, 1987; *Della Vedova* et al., 1989) indicating the presence of a thick mafic (likely gabbroic) body just underneath the sedimentary succession; (ii) logs from commercial boreholes having recovered gabbro and peridotite fragments in the deepest parts of the Gela Nappe (*Longaretti*, 1986, personal communication: see Fig. 9); (iii) oil wells in the Ragusa area, south-western part of the Hyblean Plateau, having reached tholeiite gabbros and dolerites underneath Triassic dolomite, with no evidence of pyrometamorphism, about 2500 m below sea level (*Cristofolini*, 1966 and therein references).

The above documentation suggests that the Hyblean sedimentary succession stands upon gabbroic bodies. Thus, it appears improbable that the ascending magma has sampled the bottom (upper mantle, granulitic lower crust) and top (gabbro, sedimentary sequence) of the lithospheric column, but left the middle untouched. Hence we can reasonably assume that the studied xenoliths adequately represent the Hyblean crustal basement, which may consist of a ''fossil'' peridotite-gabbro ridge (Fig. 9). Nevertheless, in case the above assumption is not agreed, the continental nature of the Hyblean lithosphere cannot be definitively ruled out.

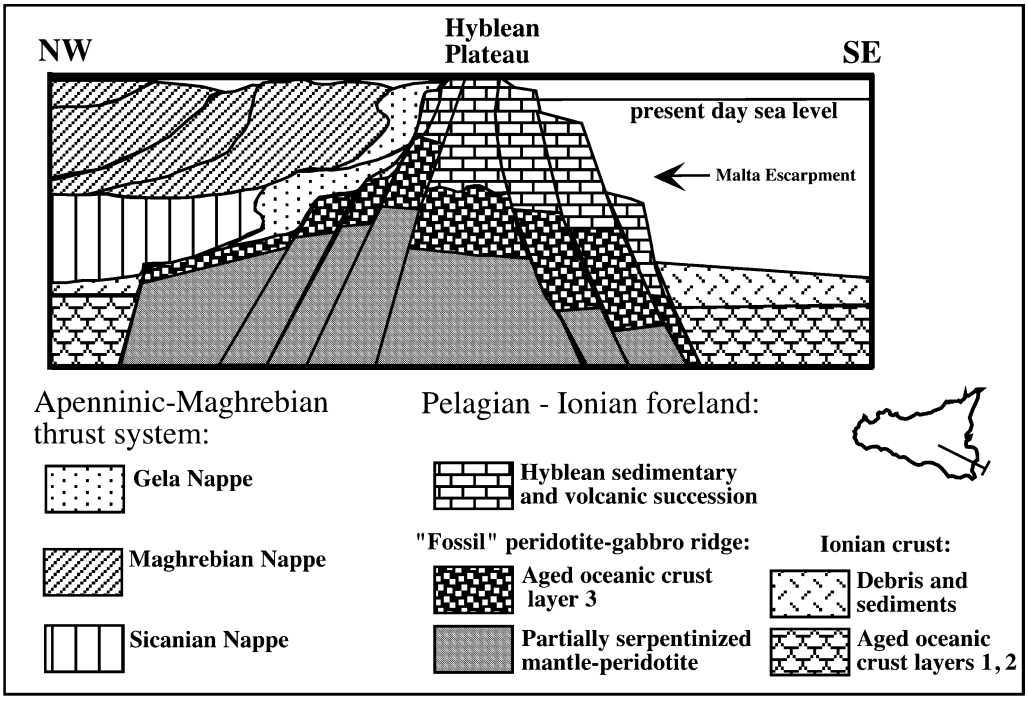

Fig. 9. Hypothetical NW–SE profile of the crustal structure across the Hyblean Plateau and neighbouring areas, according to the conclusions of the present study. Heights are exaggerated for clarity. All parts of this xenolith-based profile are merely conceptual and not to scale

Although the petrology of the xenoliths fits either an oceanic or ocean-continent-transition (OCT) nature for the peridotite/gabbro ridge, the oceanic hypothesis is more appropriate, because the xenolith-bearing diatremes are located well within the Plateau, up to 35 km from the Malta escarpment, on its land-side (Fig. 1). A supposed OCT section would, instead, have been placed on the sea-side of the slope, like the present-day Galicia and Gorringe Banks, West Iberia Margin (*Cornen* et al., 1999).

The conclusion that the lower crust beneath the Hyblean Plateau may not belong to the African continental crust, as commonly considered in the literature (*Burollet* et al., 1978), could have important implications for the geological setting of this area and, more generally, this hypothesis raises further questions concerning the geodynamic reconstruction of the Central Mediterranean area. The Hyblean lower crust may represent, like the adjacent Ionian crust, a relic of the Permo-Triassic Palaeo-Tethys ocean (*Vai*, 1994). On these grounds, the Malta escarpment, generally considered an ancient passive continental margin (*Finetti*, 1982), may instead represent a ''fossil'' segment of a transform margin.

Acknowledgements

This research was supported by MIUR funds (Progetti di Ateneo, Università di Catania, es. 2001–03) and by MIUR ex60% grants (Università di Bologna). Constructive criticism and suitable suggestions by *H. Downes* and *A. Berger* are gratefully acknowledged.

References

Anders E, Grevesse N (1989) Abundances of the elements; meteoritic and solar. Geochim Cosmochim Acta 53: 197–214

Arisi Rota F, Fichera F (1987) Magnetic interpretation related to geo-magnetic provinces: the Italian case history. Tectonophysics 138: 179–196

Beccaluva L, Siena F, Coltorti M, Di Grande A, Lo Giudice A, Macciotta G, Tassinari R, Vaccaro C (1998) Nephelinitic to tholeiitic magma generation in a transtentional tectonic setting: an integrated model for the Iblean volcanism, Sicily. J Petrol 39: 1–30

Bianchi F, Carbone S, Grasso M, Invernizzi G, Lentini F, Longaretti G, Merlini S, Moscardini F (1987) Sicilia orientale: Profilo geologico Nebrodi-Iblei. Mem Soc Geol Italiana 38: 429–458

Bianchini G, Bell K, Vaccaro C (1999) Mantle sources of the Cenozoic Iblean volcanism (SE Sicily, Italy): Sr–Nd–Pb isotopic constraints. Mineral Petrol 67: 213–222

Burollet FP, Mugniot JM, Sweeney P (1978) The geology of the Pelagian Block: the Margins and Basins of Southern Tunisia and Tripolitania. In: *Nairm AEM, Kanes WH, Stehli FG* (eds) The Ocean Basins and Margins. The Western Mediterranean. Plenum Press, New York, pp 331–359

Carbone S, Lentini F (1981) Caratteri deposizionali delle vulcaniti del Miocene superiore negli Iblei (Sicilia sud-orientale). Geol Romana 20: 79–101

Carrozzo MT, Collella P, Luzio D, Margotta C, Quarta T (1998) Interpretazione comparata sismica e gravimetrica lungo i profili C.Tindari-Gela e Marsala-Capo Passero. Atti del 6° Convegno GNGTS, Roma, pp 1075–1094

Catalano R, Franchino A, Merlini S, Sulli A (2000) A crustal section from the Eastern Algerian basin to the Ionian ocean (Central Mediterranean). Mem Soc Geol Italiana 55: 71–86

Cawthorn RG (1996) Layered intrusions. Elsevier, Amsterdam

Chironi C, De Luca L, Guerra I, Luzio D, Moretti A, Vitale M, Sea Land Group (2000) Crustal structures of the Southern Tyrrhenian Sea and Sicily Channel on the basis of the M25, M26, M28, M39, WARR profiles. Boll Soc Geol Italiana 119: 189–203

Ciminale M, Wasowski J (1989) A 3D interpretation of the aeromagnetic data of Sicily: possible tectonic implications. Ann Tectonicae 3: 140–146

Coogan L, MacLeod CJ, Dick HJB, Edwards SJ, Kvassnes A, Natland JH, Robinson PT, Thompson G, O'Hara MJ (2001) Whole-rock geochemistry of gabbros from the Southwest Indian Ridge: constraints on geochemical fractionation between the upper and lower oceanic crust and magma chamber processes at (very) slow-spreading ridges. Chem Geol 178: 1–22

Cornen G, Girardeau J, Monnier C (1999) Basalts, underplated gabbros and pyroxenites record the rifting process of the west Iberian margin. Mineral Petrol 67: 111–142

Costa S, Caby R (2000) Evolution of the Ligurian Tethys in the western Alps: Sm/Nd and U/Pb geochronology and rare-earth element geochemistry of the Montgenèvre ophiolite (France). Chem Geol 175: 449–466

Cristofolini R (1966) Le manifestazioni eruttive basiche del Trias Superiore nel sottosuolo di Ragusa (Sicilia sud-orientale). Period Mineralogia 35: 1–28

Cristofolini R, Albini A, Di Girolamo P, Stanzione D (1981) Geochemistry of some volcanic rocks from south eastern Sicily: rare earth and other trace element distribution. Bull Volcanol 44: 95–107

Della Vedova B, Pellis G, Pinna E (1989) Studio geofisico dell'area di transizione tra il Mar Pelagico e la Piana Abissale dello Jonio. Atti 8° Convegno GNGTS, pp 543–558

Desmurs L, Müntener O, Manatschal G (2002) Onset of magmatic accretion within a magma-poor rifted margin: a case study from the Platta ocean-continent transition, eastern Switzerland. Contrib Mineral Petrol 144: 365–382

Dewey JF, Cande SC, Pitman WC (1989) Tectonic evolution of the India/Eurasia collision zone. Eclogae Geol Helv 82: 717–734

Downes H (1993) The nature of the lower continental crust of Europe: petrological and geochemical evidence from xenoliths. Phys Earth Planet Interiors 179: 195–218

Dubinska E, Bylina P, Kozlowski A, Dörr W, Nejbert K, Scastock J, Kulicki C (2004) U–Pb dating of serpentinization: hydrothermal zircon from a metasomatic rodingite shell (Sudetic ophiolite, SW Poland). Chem Geol 203: 183–203

Embey-Isztin A, Downes H, Kempton PD, Dobosi G, Thirlwall M (2003) Lower crustal granulite xenoliths from the Pannonian Basin, Hungary, part 1. Mineral chemistry, thermobarometry and petrology. Contrib Mineral Petrol 144: 652–670

Finetti I (1982) Structure, stratigraphy and evolution of central Mediterranean. Boll Geofis Teor Appl 24: 247–426

Geisler T, Pidgeonm RT, van Bronswijkc W, Kurtza R (2002) Transport of uranium, thorium, and lead in metamict zircon under low-temperature hydrothermal conditions. Chem Geol 191: 141–154

Grasso M, Reuther CD (1988) The western margin of the Hyblean Plateau: a neotectonic transform system on the SE Sicilian foreland. Ann Tectonicae 2: 107–120

Hyndman RD, *Peacock SM* (2003) Serpentinization of the forearc mantle. Earth Planet Sci Lett 212: 417–432

Hofmann AW (1988) Chemical differentiation of the Earth: the relationship between mantle, continental crust and oceanic crust. Earth Planet Sci Lett 90: 297–314

Hunter RH (1996) Texture development in cumulate rocks. In: *Cawthorn RG* (ed) Layered intrusions. Elsevier, Amsterdam, pp 77–102

Kempton PD, Harmon RS (1992) Oxygen isotope evidence for large-scale hybridisation of the lower crust during magmatic underplating. Geochim Cosmochim Acta 56: 971–986

Kempton PD, Downes H, Sharkov EV, Vetrin VR, Ionov DA, Carswell DA, Beard A (1995) Petrology and geochemistry of xenoliths from the Northern Baltic shield: evidence for partial melting and metasomatism in the lower crust beneath an Archean terrane. Lithos 36: 157–184

Leake BE, Woolley AR, Arps CES, Birch WD, Gilbert MC, Grice JD, Hawthorne F, Kato A, Kisch HJ, Krivovichev VG, Linthout K, Laird J, Mandarino JA, Maresch WV, Nickel EH, Rock NMS, Schumacher JC, Smith DC, Stephenson NCN, Ungaretti L, Whittaker EJW, Youzhi G (1997) Nomenclature of amphiboles: report of the Subcommittee on Amphiboles of the International Mineralogical Association, Commission on New Minerals and Mineral Names. Am Mineral 82: 1019–1037

Lentini F, Carbone S, Catalano S, Grasso M (1996) Elementi per la ricostruzione del quadro strutturale della Sicilia orientale. Mem Soc Geol Italiana 51: 179–195

le Roex AP (1987) Source regions of mid-ocean ridge basalts: evidence for enrichment processes. In: *Menzies MA, Hawkesworth CJ* (eds) Mantle metasomatism. Academic Press, London, pp 389–422

le Roux PJ, le Roex AP, Schilling J-G, Shimizu N, Perkins WW, Pearce NJG (2002) Mantle heterogeneity beneath the southern Mid-Atlantic Ridge: trace element evidence for contamination of ambient asthenospheric mantle. Earth Planet Sci Lett 203: 479–498

Mazzoleni P, Scribano V (1994) Preliminary geochemical information on selected upper-mantle and lower-crust xenoliths from Hyblean Plateau (South Eastern Sicily). Mineral Petrogr Acta 37: 295–305

Neumann E-R, Sørensen VB, Simonsen SL, Johnsen K (2000) Gabbroic xenoliths from La Palma, Tenerife and Lanzarote, Canary Islands: evidence for reactions between mafic alkaline Canary Islands melts and old oceanic crust. J Volcanol Geotherm Res 103: 313–342

Nimis P, Vannucci R (1995) An ion microprobe study of clinopyroxenes in websteritic and megacrystic xenoliths from Hyblean Plateau (SE Sicily, Italy): constraints on HFSE/REE/Sr fractionation at mantle depth. Chem Geol 124: 185–197

Niu Y, Gilmore T, Macie S, Greig A, Bach W (2002) Mineral chemistry, whole-rock compositions, and petrogenesis of Leg 176 gabbros: data and discussion. In: *Natland JH, Dick HJB, Miller DJ, Von Herzen RP* (eds) Proceedings of the Oceanic Drilling program. Scientific Results 176, pp 1–70

Pognante U, Lombardo B, Venturelli G (1983) Petrology and geochemistry of Fe–Ti gabbros and plagiogranites from the Western Alps ophiolites. Ofioliti 8: 191–195

Pompilio M, Scribano V (1992) Nature and evolution of crystalline basement beneath the Hyblean Plateau (Sicily) inferred from xenoliths in volcanic rocks. IGCP no 276, Newsletter 5: 381–390

Punturo R (1999) Caratterizzazione petrologica e petrofisica di xenoliti di origine profonda nelle tufo-brecce mioceniche della Valle Guffari (Altopiano Ibleo, Sicilia). Thesis, Università degli studi di Catania

Punturo R, Kern H, Scribano V, Atzori P (2000) Petrophysical and petrological characteristics of deep-seated xenoliths from Hyblean Plateau, south-eastern Sicily, Italy: suggestions for a lithospheric model. Mineral Petrogr Acta 43: 1–20

Rivalenti G, Rossi A, Siena F, Sinigoi S (1984) The layered series of the Ivrea-Verbano igneous complex, Western Alps, Italy. Tschermaks Mineral Petrogr Mitt 33: 77–99

Romano R, Villari L (1973) Caratteri petrologici e magmatologici del vulcanismo ibleo. Rend Soc Italiana Mineral Petrol 29: 453–484

Ross K, Elthon D (1993) Cumulates from strongly depleted mid-ocean-ridge basalts. Nature 365: 826–829

Rudnick RL (1992) Xenoliths-Samples of the lower continental crust. In: *Fountain DM, Arculus R, Kay R* (eds) Continental Lower Crust. Elsevier, Amsterdam, pp 269–316

Salters VJM, Shimizu N (1988) World-wide occurrence of HFSE-depleted mantle. Geochim Cosmochim Acta 52: 2177–2182

Sapienza G, Scribano V (2000) Distribution and representative whole-rock chemistry of deep-seated xenoliths from the Iblean Plateau, South-Eastern Sicily, Italy. Period Mineral 69: 185–204

Schminke H-U, Klügel A, Hansteen TH, Hoernle K, Van den Bogaard P (1998) Samples from the Jurassic ocean crust beneath Gran Canaria, La Palma and Lanzarote (Canary Islands). Earth Planet Sci Lett 163: 343–360

Scribano V (1987) The ultramafic and mafic nodule suite in a tuff-breccia pipe from Cozzo Molino (Hyblean Plateau, SE Sicily). Rend Soc Italiana Mineral Petrol 42: 203–217

Scribano V (1988) Petrological notes on lower-crustal nodules from Hyblean Plateau (Sicily). Period Mineral 57: 41–52

Scribano V, Ioppolo S, Sapienza G, Calvari S (2003) Ipotesi sull'origine dei feldispati alcalini di alcuni xenoliti crostali degli Iblei. Bollettino Accademia Gioenia di Scienze Naturali, Catania 36: 5–21

Staudigel H, Muehlenbachs K, Richardson SH, Hart SR (1981) Agents of low temperature ocean crust alteration. Contrib Mineral Petrol 77: 150–157

Sun SS (1980) Lead isotopic study of young volcanic rocks from mid-ocean ridges, ocean islands and island arcs. Phil Trans R Soc Edinburgh 297: 409–445

Tiepolo M, Tribuzio R, Vannucci R (1997) Mg- and Fe-gabbroids from Northern Appennine ophiolites; parental liquids and igneous differentiation process. Ofioliti 22: 57–69

Tonarini S, D'Orazio M, Armenti P, Innocenti F, Scribano V (1996) Geochemical features of Eastern Sicily lithosphere as probed by Hyblean xenoliths and lavas. Eur J Mineral 8: 1153–1173

Tribuzio M, Messiga B, Vannucci R, Bottazzi P (1995) Trace element redistribution in high-temperature deformed gabbros from East Ligurian ophiolites (Northern Apennines, Italy): constrains on the origin of syndeformation fluids. J Metamorph Geol 13: 367–377

Tribuzio R, Tiepolo M, Vannucci R, Bottazzi P (1999) Trace element distribution within olivine-bearing gabbros from the Northern Apennine ophiolites (Italy); evidence for post-cumulus crystallization in MOR-type gabbroic rocks. Contrib Mineral Petrol 134: 123–133

Trua T, Esperança S, Mazzuoli R (1998) The evolution of the lithospheric mantle along the N. African Plate: geochemical and isotopic evidence from the tholeiitic and alkaline volcanic rocks of the Hyblean plateau, Italy. Contrib Mineral Petrol 131: 307–322

Vai GB (1994) Crustal evolution and basement elements in the Italian area: palaeogeography and characterization. Boll Geofis Teor Appl 36: 411–434

Vard E, William-Jones AE (1993) A fluid inclusion study of vug minerals in dawsonite-altered phonolite sills, Montreal, Quebec: implications for HFSE mobility. Contrib Mineral Petrol 113: 410–423

Vissers RLM, Nicolas A (1995) Mantle and lower crust exposed in oceanic ridges and in ophiolites. Kluwer, Dordrecht, pp 214

Weaver B, Tarney J (1984) Empirical approach to estimating the composition of the continental crust. Nature 310: 575–577

Wilshire HG, McGuire AV (1996) Magmatic infiltration and melting in the lower crust and upper mantle beneath the Cima volcanic field, California. Contrib Mineral Petrol 123: 358–374

Zingg A (1990) The Ivrea crustal cross-section (northern Italy and southern Switzerland). In: Exposed cross-Sections of the continental Crust NATO ASI SERIES, Series C: Mathematical and Physical Sciences 317, pp 1–19

Authors' addresses: *V. Scribano* (corresponding author; e-mail: scribano@unict.it), Dipartimento di Scienze Geologiche, Università di Catania, Corso Italia 55, 95129 Catania, Italy; *G. Sapienza* (e-mail: sapienza@geomin.unibo.it), *R. Braga* (e-mail: braga@geomin.unibo.it), and *L. Morten* (e-mail: morten@geomin.unibo.it), Dipartimento di Scienze della Terra e Geologico-Ambientali, Università di Bologna, Piazza di Porta S. Donato 1, 46126 Bologna, Italy